J Mater Sci (2010) 45:5624–5636
DOI 10.1007/s10853-010-4627-9

Effect of annealing on precipitation, microstructural stability, and mechanical properties of cryorolled Al 6063 alloy

Sushanta Kumar Panigrahi · R. Jayaganthan

Received: 13 December 2009 / Accepted: 17 May 2010 / Published online: 3 June 2010

Abstract The effect of annealing on precipitation, microstructural stability, and mechanical properties of cryorolled Al 6063 alloy has been investigated in the present work employing hardness measurements, tensile test, XRD, DSC, EBSD, and TEM. The solution-treated bulk Al 6063 alloy was subjected to cryorolling to produce ultrafine grain structures and subsequently annealing treatment to investigate its thermal stability. The CR Al 6063 alloys with ultrafine-grained microstructure are thermally stable up to 250 °C as observed in the present work. Within the range of 150–225 °C, the size of small precipitate particles is <1 μm. These small precipitate particles pin the grain boundaries due to Zener drag effect, due to which the grain growth is retarded. The hardness and tensile strength of the cryorolled Al 6063 alloys have decreased upon subjecting it to annealing treatment (150–250 °C).

Introduction

Aluminum alloys (6XXX series) are widely used in the structural components of automotive and construction industries as they show a good combination of formability, corrosion resistance, weldability, and final mechanical properties [1]. They represent the highest volume (90%) of the western world extruded aluminum products [2, 3] and usage of these alloys in various sectors has grown more than 80% within a span of 5 years [4]. It is well known that about 46% of aluminum alloys used for various applications is in the form of sheets and plates [5]. An increased usage of these alloys depends on enhancing their mechanical properties such as strength and toughness further. The grain refinement of bulk Al alloys to ultrafine regime can further enhance its mechanical properties. Hence, cryorolling has been identified as one of the potential routes to produce ultrafine-grained (UFG) materials from its bulk alloys [6].

UFG materials produced by cryorolling and other severe plastic deformation processes have attracted much attention from material scientists due to their excellent strength [6–10]. A comparatively lower strain induced in the materials by cryorolling is sufficient to produce the UFG microstructure than the existing SPD techniques. Kim et al. [11] and Kwan et al. [12] have developed UFG Al alloys at the equivalent true strain of 8 and 6.6 using equal channel angular pressing and accumulative roll bonding, respectively. However, UFG Al 6063 alloy is developed at the true stain of 3.6 by cryorolling as reported in our earlier work [9]. Available experimental and theoretical studies attribute the low ductility of nanostructured and UFG materials to the reduced dislocation activity [13]. Due to the high energy stored in the deformed state and the presence of structural heterogeneities, these materials are not thermally stable [14, 15]. A proper annealing treatment is essential for improving the ductility as well as stabilizing the microstructure of the cryorolled materials. If the ultrafine grains are stable at temperature where the diffusion rate is rapid, it may exhibit super plasticity at high strain rates as reported in the literature [16, 17].

In recent years, majority of published work deals with the annealing behavior of the severely deformed [15, 18–20] Al and non-heat treatable Al alloys, and relatively little work has been reported on heat treatable Al alloys. The severely deformed Al–3Mg alloys subjected to low- and

S. K. Panigrahi · R. Jayaganthan (✉)
Department of Metallurgical and Materials Engineering, Indian Institute of Technology Roorkee, Roorkee 247667, India
e-mail: rjayafmt@iitr.ernet.in

high-temperature annealing treatments, caused a reduction in dislocation density and grain coarsening, and localized recrystallization in the alloy, respectively [18]. Lee et al. [19] have investigated the effect of annealing treatment on microstructures and mechanical properties of cryorolled Al 5083 alloy. The optimized cryorolling strain imparted to the samples, with subsequent annealing treatment resulted in the formation of mixture of equiaxed grains (<200 nm) and elongated sub grains, which showed a good combination of uniform elongation and high strength as reported in their work. Cao et al. [20] investigated the annealing behavior of commercial purity Al deformed by ECAP at different strains. They suggested that at low strains, recrystallization occurs in a discontinuous manner and at high strains, the recrystallization occurs by both, discontinuous and continuous manner.

The development of UFG bulk Al alloys (6XXX series) through cryorolling is very scarce in the literature. Since Al 6063 alloy is a precipitation hardenable alloy, an annealing treatment to this material after cryorolling is expected to stabilize its microstructure as well as release the second-phase precipitate particles from the matrix. It is very important to understand the influence of second-phase particles on recrystallization of the cryorolled Al 6063 alloy. An insight into the effects of these particles on annealing behavior will be beneficial to exploit the second-phase particles as a method to control the grain size and texture during thermo mechanical processing of Al alloys. During annealing, primary effect of the closely spaced particles may tend to pin the grain boundaries; however, the deformation heterogeneities at large particles may act as sites for the occurrence of recrystallization [21].

Recently, the annealing behavior of cryorolled materials such as Cu, Al, Al 5083 alloy has been studied in detail [6, 19, 22]. On the other hand, the annealing behavior of cryorolled Al 6XXX series has received limited attention so far. Owing to the aforementioned views, the objectives of the present work are: (i) to study the effect of annealing on precipitation behavior of cryorolled (CR) Al 6063 alloy; (ii) to study the effect of annealing on microstructure and mechanical properties of this CR alloy; and (iii) to analyze the influence of second-phase precipitate particles on recrystallization behavior of the CR alloy.

Experimental

The Al 6063 alloy plates (9.6 mm) of T4 temper treated, with the compositions of 0.45% Si, 0.3% Mg, 0.015% Cu, 0.013% Mn, 0.058% Fe, 0.022% Zn, 0.02% Cr (wt%) were procured from the Hindalco Industries Ltd, Aditya Birla Group, Renukoot, India for the present work. These plates were solution-treated (ST) at 520 °C for 1 h and then quenched in water. The ST Al 6063 alloy plates were then cryorolled (CR) up to a true strain of 2.3. In cryorolling, the Al 6063 alloy plates are rolled at liquid nitrogen temperature. The materials are dipped in liquid nitrogen for 30 min, before rolling, and it was repeated for each successive rolling pass. The process was continued until imparting the true strain of 2.3 to the sample. The diameter of the rolls and its speed were 110 mm and 8 rpm, respectively.

The CR Al alloy sheets were subjected to annealing treatment at various temperatures in the range of 50–300 °C for duration of 1 h for improving ductility as well as for investigating the thermal stability. The microstructural features of the CR Al 6063 alloy samples during annealing at different temperatures were examined in detail by EBSD and TEM analyses. The samples for electron back scattered diffraction (EBSD) characterization were prepared by mechanical polishing using 1000 grit emery paper, fine polishing to mirror finish with diamond paste, and then finally electro polished at −15 °C using an electrolyte of methanol/perchloric acid (80:20) at 11 V of dc power source. The EBSD measurements were performed at the center of the samples with a scan area of 6 μm × 8 μm. The step size of 0.1 μm was used during the measurements. TSL OIM analysis 4.6 software developed by TEXSEM Laboratories Inc. was used to analyze the EBSD maps. Microstructural characterization of the CR materials was carried out in a FEI Technai 20 transmission electron microscope (TEM) operated at 200 kV. For TEM study, the samples were prepared by mechanical grinding to a thickness of 0.15 mm and then thinning by a twin-jet electro polishing unit with a solution of 20-pct nitric acid and 80-pct methanol at a temperature of −30 °C. X-ray diffraction (XRD) (Bruker AXS D8 Advance instrument) analysis using Cu Kα radiation was carried out to identify the formation of different phases of the CR samples subjected to different annealing treatments. The thermal behaviors of CR samples with different annealing treatments were evaluated using a Perklin Elmer paris Diamond DSC under pure nitrogen atmosphere at the rate of 100 mL/min. A sample weighing approximately 30 mg (5-mm diameter and 0.8-mm thickness) was placed in one of the pans in DSC and the other pan was used for aluminum reference. In order to increase sensitivity of the instrument, the base line correction was made. The DSC run was carried out at a heating rate of 20 °C/min and the measurements were performed at least two times for each of the different samples, which result in good reproducibility.

Microhardness and tensile tests were carried out to evaluate the strength and ductility of the cryorolled Al 6063 alloy samples subjected to the different annealing treatments. Vickers micro hardness (*Hv*) was measured on the plane parallel to longitudinal axis (rolling direction) by

applying a load of 100 g for 15 s. Prior to each *Hv* measurement, the surface of the specimen was polished mechanically using emery paper and diamond paste of 0.25 μm to ensure its clean surface. The reported micro hardness value is based on the average of ten measurements made on the surface of each specimen.

The tensile specimens were machined as per ASTM E-8 sub-size specifications parallel to the rolling direction with gauge length of 25 mm. The tensile tests were performed after polishing the samples in air at room temperature using a S-Series, H25K-S materials testing machine operated at a constant crosshead speed with an initial strain rate of 5×10^{-4} S^{-1}. The tensile samples after rolling had the same length and width but a different thickness in accordance with rolling reductions.

Results

XRD analysis

The X-ray diffraction patterns of CR Al 6063 alloy at different annealing temperatures are shown in Fig. 1. It does not show any formation of Mg_2Si precipitate peak but the peak pertaining to precipitation is observed in CR samples subjected to annealing treatment at all temperatures. The intensity of Mg_2Si precipitate is observed to be low for the CR samples subjected to the annealing treatment at low temperatures; however, the intensity becomes sharper for the CR samples subjected to high-temperature annealing treatments.

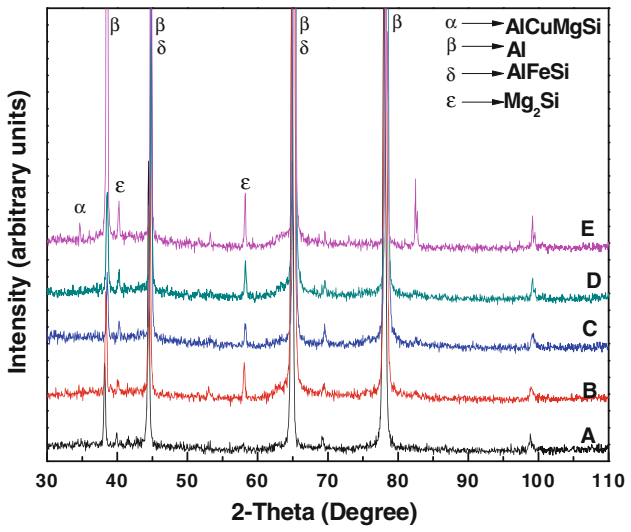

Fig. 1 XRD patterns of CR Al 6063 alloy samples annealed at different temperatures for 1 h; (A) 0 °C, (B) 150 °C, (C) 200 °C, (D) 225 °C, and (E) 250 °C

DSC analysis during annealing

The DSC curves, for ST samples, obtained at a heating rate of 20 °C/min before cryorolling are represented in Fig. 2a, which shows five exothermic peaks and two endothermic peaks. The exothermic reaction peak 1 at a temperature range of 65–125 °C represents the formation of solute-rich clusters. The formation of GP-zones or Si–Mg-vacancy clusters (peak 2) is observed at a temperature range of 145–200 °C; the endothermic peak 2_a (200–230 °C) may be attributed to the dissolution of the preformed clusters/GP zones. The formation of coherent precipitate β'' and incoherent precipitate β' are observed at the peak temperature range of 235–285 °C (peak 3) and 290–315 °C (peak 4), respectively. The dissolution peak of β' (peak 4_a) occurred at the range of 335–360 °C and

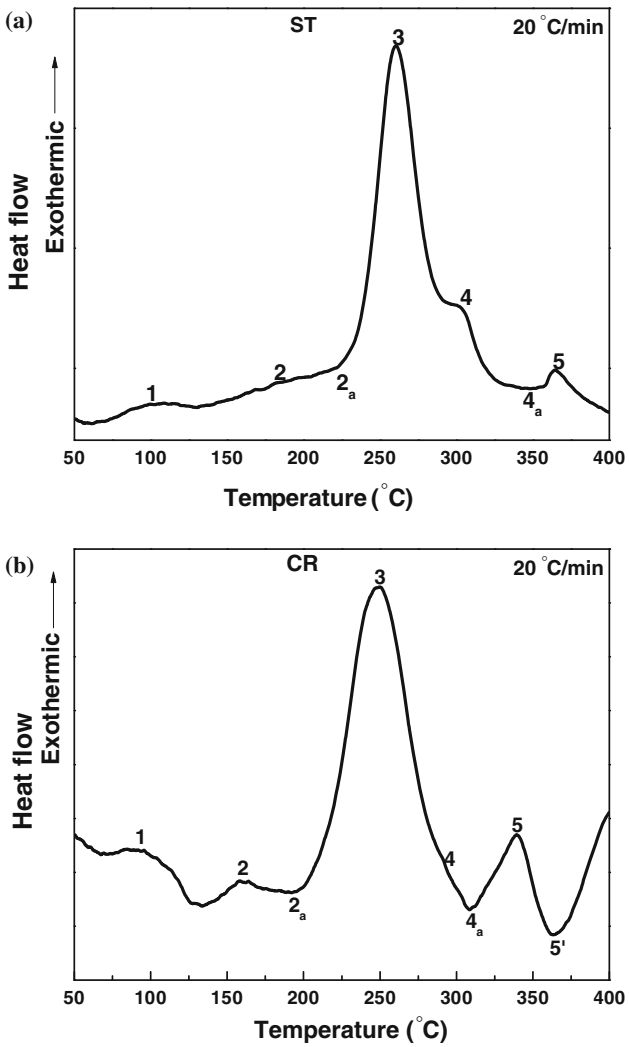

Fig. 2 DSC plot of ST and CR Al 6063 alloy samples at a heating rate of 20 °C/min **a** ST sample, **b** CR sample

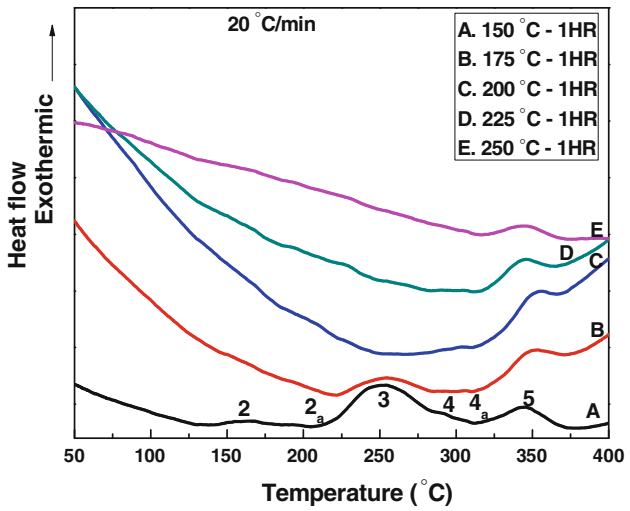

Fig. 3 DSC plots of CR Al 6063 alloy after annealing at different temperatures

the formation of equilibrium β (peak 5) occurs at the range of 360–380 °C. The trend of precipitation kinetics is in accordance with the published literature on similar alloys [8, 23, 24]. The DSC curves of the CR sample obtained at a heating rate of 20 °C/min before annealing treatment are shown in Fig. 2b. All the reaction peaks corresponding to the formation and dissolution of different precipitate reactions of CR samples were shifted toward left when compared to the samples before cryorolling. Also, the precipitate reaction peaks which were observed in the ST samples before cryorolling are still retained after cryorolling.

The precipitate evolutions during the isothermal annealing of CR samples at 150–250 °C were studied in detail by DSC and shown in Fig. 3. All the exothermic and endothermic reaction peaks as observed in the CR sample are still found in the CR samples after annealing at 150 °C for 1 h except peak 1(formation of clusters). However, intensity of the peaks corresponding to formation of GP zones and β'' precipitate is less. At an annealing treatment of 175 °C, intensity of the peaks corresponding to the formation of GP zones and β'' precipitate is reduced. However, there is no change in the intensity of the remaining peaks such as formation of β' precipitate and stable β precipitate. The similar precipitation behavior is observed at the annealing temperatures of 200 and 225 °C. The peak corresponding to stable β precipitate is clearly observed in both the annealing conditions. A small intensity peak of β' precipitate is also observed in both the cases. None of the precipitate peaks except a stable peak corresponding to β precipitate is observed in the CR samples subjected to the annealing treatment at 250 °C.

TEM study

In order to study the effect of annealing on precipitation behavior of CR Al 6063 alloy samples, the microstructures of CR samples at different annealing treatments were characterized using high-resolution transmission electron microscopy (HRTEM) and their corresponding images are shown in Fig. 4. The presence of spherical and needle-shaped particles is observed in the CR samples after annealing at a temperature of 150 °C (Fig. 4a). However, the volume fraction of spherical particles is more as compared to that of needle-shaped particles. The diameter of all the spherical particles is found to be within the range of 5–10 nm. The XRD results (Fig. 1B) show the peak pertaining to the formation of Mg_2Si precipitate in this annealing treatment. As per the DSC results (Fig. 3A), the intensity of the peak corresponding to formation of GP zones, and β'' precipitate is comparatively lesser than that of CR samples without annealing treatment. These results confirm that the spherical particles and needle-shaped particle as observed in the TEM microstructure are GP zones and β'' precipitate particles, respectively. The morphology of GP zones (spherical) as seen from the TEM micrograph (Fig. 4a) agrees well with the results observed by Miao et al. [23].

The CR samples subjected to an annealing temperature of 175 °C contain the spherical and needle-shaped particles as shown in HRTEM micrograph (Fig 4b). The volume fraction of needle-shaped particles is more as compared to that of spherical particles. Most of the needle-shaped particles are lying in the range of 15–60 nm in length and 5–10 nm in diameter. The DSC result (3B) shows the absence of GP zones. The intensity of the peak corresponding to the formation of β'' precipitate is also reduced. This clearly indicates that at this annealing temperature, the β'' precipitates emerges out from the solid solution and retained in the microstructure. So, when the samples containing β'' precipitate particles are further annealed in DSC instrument, the intensity of the peak corresponding to the formation of β'' precipitates is reduced. Therefore, it is confirmed that the needle-shaped particles as observed from the TEM microstructure are β'' precipitate particles. The observed morphology of β'' precipitates (needle shaped) (Fig. 4b) in the present work correlates well with the results observed by other researchers [23, 25].

Figure 4c shows the precipitate morphology of the CR samples after annealing at a temperature of 200 °C. The microstructure contains, mostly rod-shaped particles. The rods are lying within the range of 15–25 nm in diameter and 250 nm to 2 μm in length. The XRD results (Fig. 1C) confirm the presence of these rods as the Mg_2Si precipitate particles. It is observed from DSC results (Fig. 3C) that the precipitate peak corresponds to the formation of β'

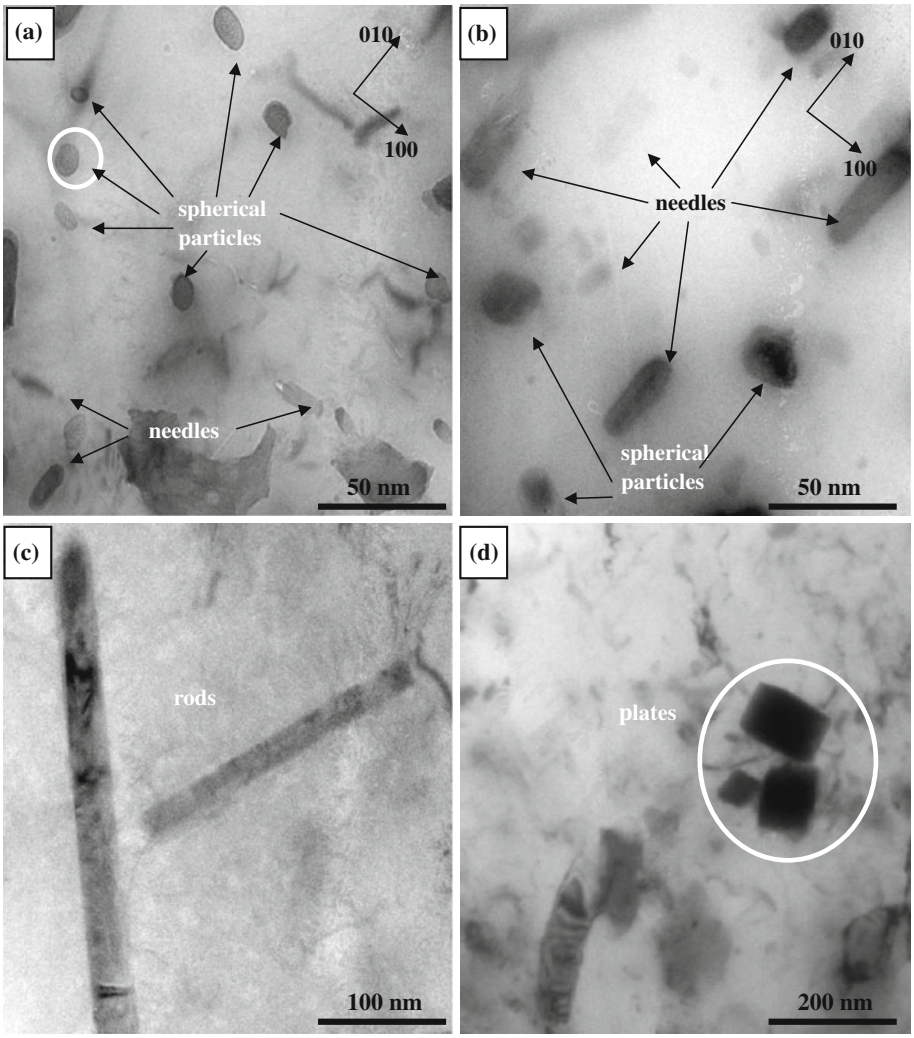

Fig. 4 HRTEM images of CR Al 6063 alloy samples annealed at different temperatures for 1 h; **a** 150 °C, **b** 175 °C, **c** 200 °C, and **d** 250 °C

precipitates. However, a full intensity of peak pertaining to β' precipitate formation and a small intensity peak for β'' precipitate formation is observed at the annealing treatment of 175 °C. Hence, at an annealing treatment of 200 °C, the transformation of β'' to β' phase might have occurred. Therefore, the rod-shaped particles as seen from TEM microstructure might be β' precipitate particles. The morphology of β' precipitates as observed in the present work is in tandem with the results obtained by other researchers [26, 27].

When the CR samples are annealed at 225 °C, the precipitation evolution, observed from XRD and DSC results, appear similar to the CR samples annealed at 200 °C. Hence, TEM investigation was not conducted at this annealing treatment by assuming that similar kind of β' precipitate particles might be observed in the microstructure.

The TEM images of the CR sample annealed at a temperature of 250 °C is shown in Fig. 4d. The presence of spherical particles, needle-shaped, or rod-shaped particles which were seen at lower annealing treatments are not observed in this annealing treatment (250 °C) even at high magnification. In low-magnification TEM microstructures, few plate-shaped particles are observed (Fig. 4d). However, these plate-shaped particles are not distributed in the matrix homogeneously. The dimension of the plates falls within the range of 100–150 nm in length or width. The XRD results (Fig. 1E) confirm the presence of these plate-shaped particles as the Mg_2Si precipitate particles. The DSC plot (Fig. 3E), at this annealing treatment, is similar to that of it observed at the annealing treatment of 200 and 225 °C. However, the intensity of the peak for the formation of β precipitate is observed to be low at the annealing treatment of 250 °C. It indicates that few precipitate particles of β phase are transformed from β' phase and found in the microstructure. When the samples containing β precipitate particles in the microstructure are further annealed in DSC, the intensity of the peak corresponding to the formation of β precipitate is reduced. The DSC result confirmed that the plate-shaped particles as observed from the TEM microstructure might be the stable β precipitates.

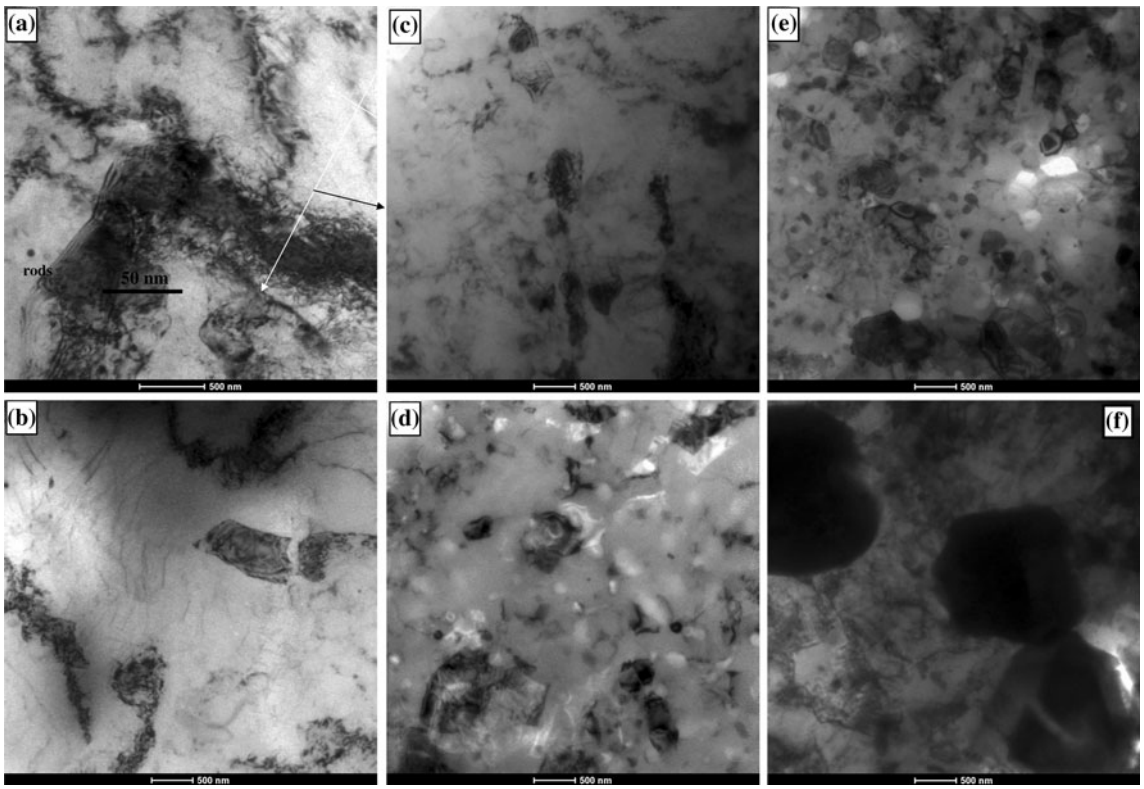

Fig. 5 TEM images of CR Al 6063 alloy samples annealed at different temperatures for 1 h; **a** 0 °C, **b** 150 °C, **c** 175 °C, **d** 200 °C, **e** 225 °C, and **f** 250 °C

The evolution of microstructure such as changes in dislocation content and subgrain morphology during isothermal annealing at temperature range of 150–250 °C are examined in detail by TEM study and shown in Fig. 5. In the CR sample without annealing treatment (Fig. 5a), a heavily deformed microstructure with diffused, non-equilibrium, and ill-defined grain boundaries was observed. Dislocation cells, dislocation-tangling zone, and dense dislocation walls were also observed in the heavily deformed grains of the CR sample. When the CR samples are annealed at 150 °C (Fig. 5b), a slight reduction of dislocation density and relaxation of cell boundaries into subgrain walls are observed. The dislocation density is rarely observed in few of the grains for the samples annealed at 175 °C (Fig. 5c). Annealing at 200 °C (Fig. 5d), led to a significant dislocation recovery. Most of the grains in this condition appear much more equiaxed than the other low-temperature annealed samples. There is no significant change in TEM microstructure when the CR samples are annealed at a temperature of 225 °C (Fig. 5e). It exhibits equiaxed grains with its size varying from 100 to 500 nm. The CR samples annealed at a temperature of 250 °C (Fig. 5f), led to coarsening in the microstructure, in which grains size has increased to 1–3 μm.

EBSD analysis during annealing

The microstructural evolution during annealing at temperatures (150–250 °C) has been examined in detail by EBSD analysis and shown in Fig. 6. The black and gray lines from the EBSD maps as shown in Fig. 6 indicate the location of high angle grain boundaries (HAB) ($\geq$15°) and low angle grain boundaries (LAB) (1.5–15°), respectively. The different gray contrast in the EBSD maps corresponds to different grain orientations. The EBSD measurements for CR samples subjected to annealing treatments were performed at the center of the samples with a step size of 0.1 μm. Figure 6a shows the EBSD microstructure of the CR samples before annealing treatment. The severely fragmented and elongated sub-grains like thin ribbon, along the rolling direction with low aspect ratio were observed. The microstructure of the CR sample subjected to an annealing treatment at a temperature of 150 °C is inhomogeneous, where some region shows relatively high density of LAB and the other region appears as elongated lamellar with UFG structure. The gray line shows the LAB, which corresponds to the dislocation substructures. The higher fractions of dislocation substructures are still present in the CR sample after the annealing treatment of

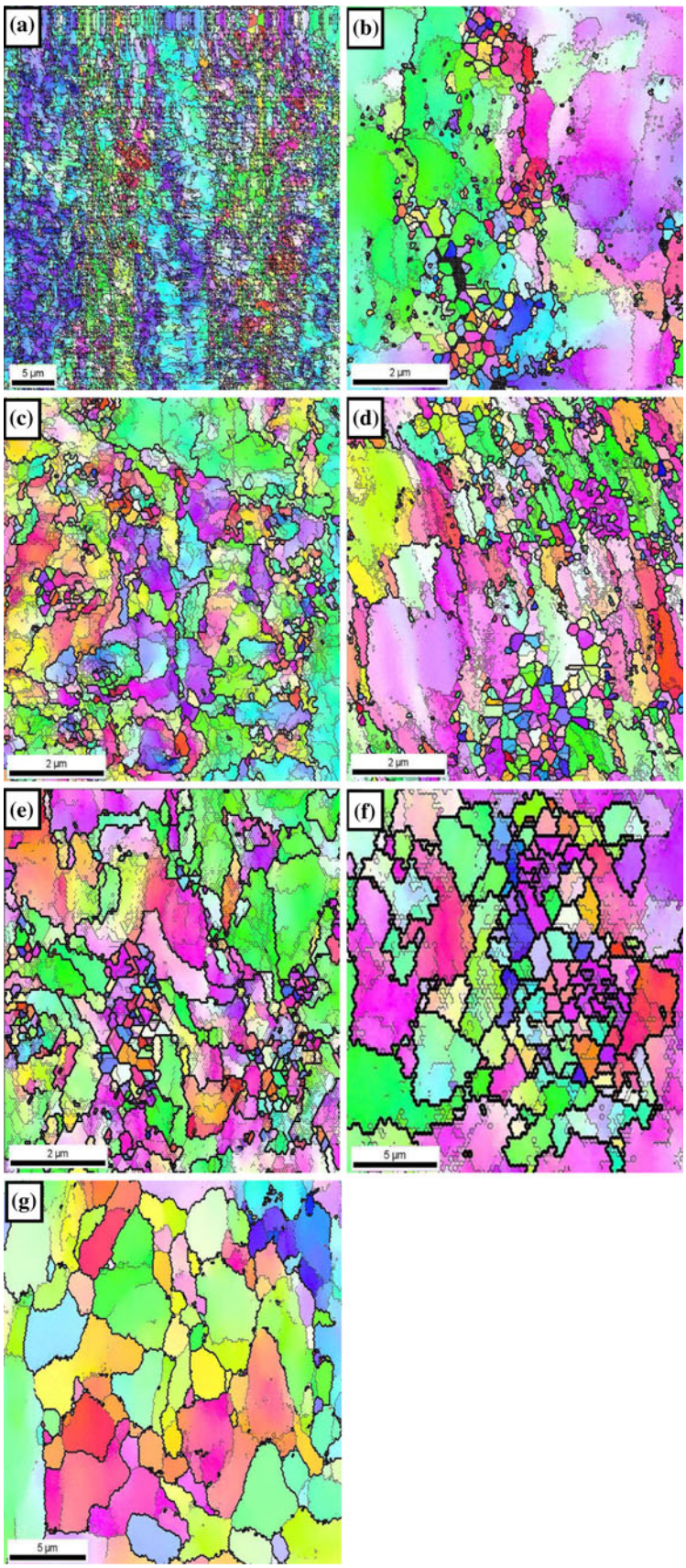

Fig. 6 EBSD micrographs of CR Al 6063 alloy samples annealed at different temperatures for 1 h; **a** 0 °C, **b** 150 °C, **c** 175 °C, **d** 200 °C, **e** 225 °C, **f** 250 °C, and **g** 300 °C

150 °C. However, the dense LAB network as observed in the CR samples before annealing is quite reduced. Some of the dislocations are rearranged themselves and transformed into formation of subgrains with clear boundaries (Fig. 6b). When the CR samples are annealed at 175 °C, two distinct features are observed from the microstructure (Fig. 6c); in one region, the equiaxed grains are homogeneously distributed with the grain size approaching 200–400 nm range and the other region contains deformed microstructure. Annealing at 200 °C (Fig. 6d) led to nucleation of equiaxed grains in many regions. In some places, the elongated grains are also observed. In the other region, the deformed structure with a LAB network is observed. The microstructure of the CR sample subjected to an annealing treatment at a temperature of 225 °C (Fig. 6e) shows the homogeneous distribution of equiaxed grains in many regions. The size of the grains in these regions lies within the range of 300–500 nm. However, a few unrecrystallized areas are still observed. The partial grain coarsening behavior is observed in microstructure of the CR sample subjected to an annealing treatment at a temperature of 250 °C. In this condition, a duplex microstructure is observed. In some regions, slightly coarsened grains with size range of 500 nm to 1 μm are observed; and in some other region, coarser grains of about 2–5 μm range are seen (Fig. 6f). At the annealing temperature of 300 °C, all the grains are coarsened within the range of 1–6 μm (Fig. 6g).

The histograms of the boundary misorientation distribution of the CR materials subjected to the annealing treatment at temperatures in the range of 150–250 °C are shown in Fig. 7. The CR material without annealing treatment shows a high fraction of LAB. When the CR samples are subjected to annealing treatment at different temperatures, the proportion of LAB is reduced but it shows higher fraction of HAB. The rate of transformation of LAB to HAB is low at annealing temperatures, such as 150, 175, and 200 °C. When the CR samples are subjected to the annealing temperatures beyond 225 °C, almost all the LAB are transformed to HAB.

Effect of annealing on mechanical properties

The influence of annealing treatment, at temperature 50–300 °C, on the mechanical properties of CR Al 6063 alloy has been studied by employing tensile test. Figure 8 and Table 1 show the tensile properties of CR Al 6063 alloy samples at different annealing temperatures. There is no change in yield strength (YS) and ultimate tensile strength (UTS), when the CR samples are subjected to a low temperature annealing treatment of 50 °C. During the annealing treatment of 50–150 °C, a gradual increase in both YS and UTS is observed. At the annealing treatment from 150 to 175 °C, a gradual decrease in both YS and UTS is observed. When the annealing temperature exceeds beyond 175 °C, a rapid drop in both tensile properties are observed up to a temperature of 250 °C. There is no change in YS and UTS between the annealing treatment range of 250–275 °C. A further decrease in both YS and UTS are observed in the CR samples after annealing beyond a temperature of 275 °C. The ductility of the CR samples improves gradually up to an annealing temperature of 175 °C. Beyond this temperature, the decrease in ductility is observed up to an annealing temperature of 200 °C and then the ductility improves drastically up to an annealing temperature of 250 °C. The ductility remains almost constant between the annealing temperatures of 250 and 275 °C; beyond this annealing temperature, the ductility improves further. The fracture strain is termed as ductility in the present case.

The effect of annealing temperature on hardness of CR samples are studied in detail and shown in Fig. 9. The trend of hardness results of the CR samples at different annealing temperatures is similar to that of the strength properties. The variation in microhardness values is small at low temperatures, followed by a rapid decline and finally levels off at higher annealing temperatures.

Discussion

Precipitate evolution during annealing

The influence of annealing on precipitate evolution of CR Al 6063 alloy has been studied by XRD, TEM, and DSC in the present work. The precipitation evolution of the CR Al 6063 alloy samples during annealing treatment in the range of 150–250 °C can be described as per the existing precipitation sequence of the bulk Al–Mg–Si alloy [28]. The precipitation sequence of this alloy after subjecting to solution treatment and quenching is as follows:

$$\alpha(\text{supersaturated solid solution}) \rightarrow \text{GP zones} \rightarrow \beta'' \rightarrow \beta' \rightarrow \beta$$

During solutionizing and quenching, the solute atoms were completely dissolved in the Al matrix and retained in metastable state. When these quenched samples were cryorolled up to a strain of 2.3, the solutes are still retained in the solid solution in metastable state. Since the samples are rolled at cryogenic temperature, the sample has not received sufficient thermal energy to precipitate the solutes from the solid solution. When the CR samples are annealed at 150 °C, the Mg and Si are clustered together and formed GP zones with spherical shape. At an annealing temperature of 175 °C, the formation of needle-shaped

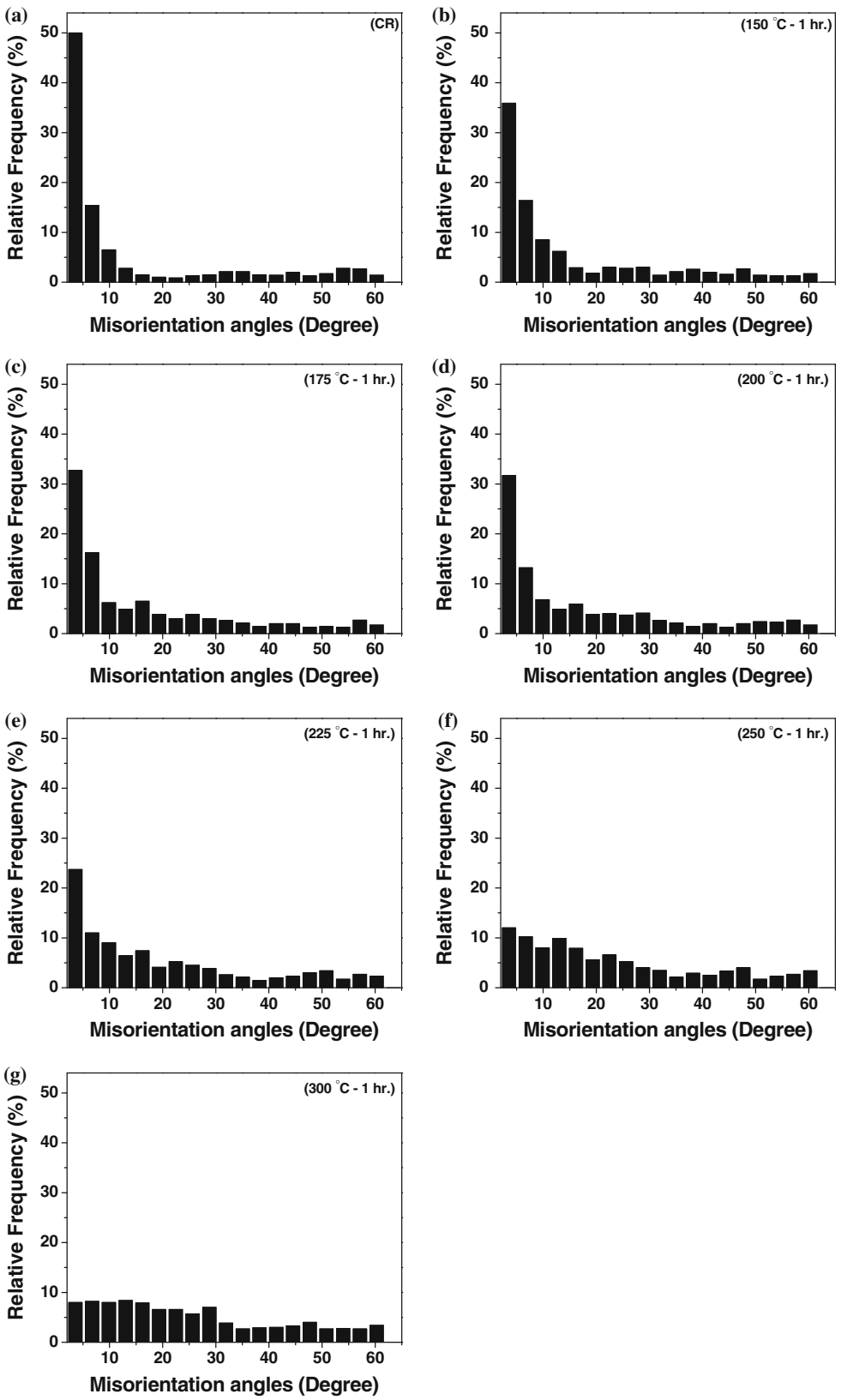

Fig. 7 Frequency histograms of CR Al 6063 alloy samples annealed at different temperatures for 1 h; **a** 0 °C, **b** 150 °C, **c** 175 °C, **d** 200 °C, **e** 225 °C, **f** 250 °C, and **g** 300 °C

precipitates of β'' phase has occurred. At 200 °C, the microstructure contains the rod-shaped β' precipitate phase. At the annealing temperature of 225 °C, the β' precipitate might have dissolved into bigger precipitate particles. At an annealing temperature of 250 °C, the plate or cube-shaped stable β phase has formed.

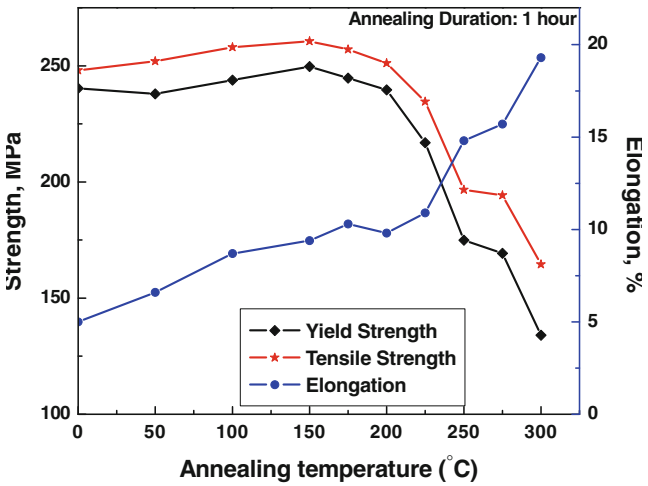

Fig. 8 The effect of annealing temperature on tensile properties of CR Al 6063 alloy

Table 1 Tensile properties of CR Al 6063 alloy at different annealing temperatures for 1-h duration

Annealing temperature (°C)	YS (MPa)	UTS (MPa)	ELONG
0	240.3	248	5
50	237.9	252	6.68
100	243.8	258	8.7
150	249.7	260.6	9.4
175	244.7	257	10.3
200	239.6	251.1	9.1
225	216.9	234.6	10.9
250	174.9	196.6	14.8
275	169.3	194.2	15.8
300	134	164.5	19

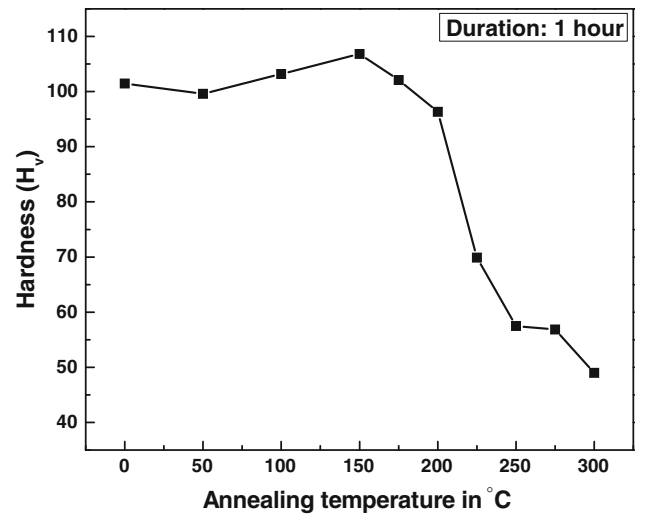

Fig. 9 The effect of annealing temperature on hardness properties of CR Al 6063 alloy

Buha et al. [29] studied the effect of aging on precipitate evolution of solution treated Al–Mg–Si alloy. They observed the formation of GP zones when the samples are aged at 177 °C for 4 h. They found the formation of other intermediate phases such as β'' phase and β' phase at the aging temperatures of 177 °C for 15 h and 177 °C for 160 h, respectively. Urrutia et al. [30] studied the aging behavior of Al 6082 alloy and found the formation of β'' phase and β' phases at the aging treatments of 250 °C for 30 min and 250 °C for 8 h, respectively. However, in the present investigation of CR Al 6063 alloy, the formation of GP zones, β'' phase, β' phase, and stable β phase are observed at the annealing temperatures of 150 °C for 1 h, 175 °C for 1 h, 200 °C for 1 h, and 250 °C for 1 h, respectively. All the intermediate precipitate phases are observed within duration of 1 h, in the present investigation. The rapid precipitation kinetics of CR strained samples as compared to the undeformed samples may be due to the presence of enhanced dislocation, which could act as a short-circuit path for solutes and atomic migration to facilitate the precipitation.

Evolution of microstructure during annealing

The CR samples, before annealing treatment, exhibit a heavily deformed microstructure with diffused, non-equilibrium, and ill-defined grain boundaries. During low-temperature annealing of the CR samples, between 150 and 175 °C, recovery occurs causing a significant reduction in dislocation density in the samples. Some of the dislocations rearrange themselves to form subgrains and many of the elongated substructure boundaries recovered into subgrain boundaries, during the recovery process.

The duplex nature of microstructure observed at an annealing temperature of 175 °C, during recrystallization, is due to heterogeneities in the deformed (cryorolled) samples. When the annealing temperature is increased to 200 °C, most of the grains are recrystallized and show equiaxed grain morphology. A homogeneous distribution of equiaxed grains is observed in the samples subjected to annealing treatment at 225 °C. The size of recrystallized grains observed in the samples, annealed at 175 °C, is in the range of 200–500 nm and it remains more or less same even at an annealing temperature of 225 °C. It is evident that there is no grain coarsening and the microstructure is stable up to an annealing temperature of 225 °C.

When the CR samples are annealed at high temperature of 250 °C, grain coarsening has occurred. At this temperature, the grains are coarsened in duplex manner such as slightly coarsened grains with size range of 500 nm to 1 μm in some region and much coarser grains of about 2–5 μm range, in other region. At the annealing temperature of 300 °C and above, all the grains are coarsened with its

size varying from 1–6 μm. The possible reasons for abnormal grain growth at high-temperature annealing (250 °C for 1 h and 300 °C for 1 h) is due to the structural instability such as low proportion of HAB observed in the cryorolled samples before annealing. Only, when fraction of the HAB in the deformed samples [31] is higher than 70%, it will be stable against abnormal grain coarsening and discontinuous recrystallization occurring at their respective annealing temperature. In the present study, only about 35% of HAB are observed in the CR samples before annealing treatment, which is not sufficient to cause continuous recrystallization at lower annealing temperature and uniform grain coarsening at higher annealing temperature. Our observation is in tandem with results obtained by Morris et al. [32].

The recrystallization behavior is normally influenced by the presence of precipitates. During annealing treatment of CR Al 6063 alloy at different temperatures, the recrystallization and precipitation occur simultaneously. It is observed that the precipitation of GP zones, β'' phase, β' phase occurs at the annealing temperatures of 175, 200, and 225 °C, respectively. The size of all these three precipitate phases is below 1 μm. The thermal stability of the CR samples up to the annealing temperature of 225 °C may be due to the Zener drag effect. At an annealing temperature of 250 °C, the plate-shaped β phase is observed, whose volume is higher than that of GP zones, β'' phase, β' phase particles. The grain boundary pinning force may become weak due to precipitate growth, which results in the migration of grain boundaries. The distribution of these plate-shaped β phase particles are not uniform. Hence, the rate of recrystallization is faster wherever these precipitate particles are present, and it is slow in the other region. This might be one of the possible reasons for the abnormal grain growth of the CR samples annealed at higher temperature.

Effect of annealing on mechanical properties

The influence of annealing on mechanical properties of CR samples has been investigated in detail by employing tensile test and hardness test. When the CR samples are subjected to annealing treatment at 150 °C, the precipitation of GP zone has occurred. These fine precipitate particles act as a barrier for dislocation movement, resulting in enhancement of initial strength and hardness. The main reason for the improvement of ductility from 5 to 9.4% is due to recovery. When the annealing temperature is increased from 150 to 175 °C, a slight reduction in the strength and hardness has occurred. The precipitation of β'' phase has occurred at 175 °C. It is reported that the β'' precipitate phase [24, 33] is the highest hardening phase as compared to other intermediate precipitates in Al–Mg–Si alloys. These β'' phase particles obstructs the dislocation movement during tensile straining, resulting in enhanced strength and hardness. However, the strength decreases due to transformation of dislocation free grains. The increase in elongation also confirms the softening behavior due to dislocation free grains. From 175 to 250 °C, a drastic decrease in tensile strength, yield strength, hardness and a significant increase in the elongation is observed. This rapid increment of softening rate indicates that the rate of recrystallization is fast during this temperature range. The hardening effect as observed during the low annealing temperatures is not observed at the temperature range of 175–250 °C. Up to the annealing temperature of 175 °C, the precipitates are coherent with the matrix, therefore higher strength and hardness were observed. When the temperature is increased beyond 175 °C, the hardening effect is lost due to the formation of incoherent precipitate particles. At the temperature above 250 °C, there is no change in yield strength, tensile strength, and hardness. It clearly indicates that the recrystallization process completes at 250 °C. The recrystallization kinetics as observed from the mechanical properties is tandem with that of microstructural evolution.

From the hardness measurements, the recrystallized fractions can be obtained by assuming a fraction recrystallized of one for low hardness value and zero for high hardness value.

It can be mathematically expressed as

$$X_i = \frac{H_{\max} - H_i}{H_{\max} - H_{\min}} \quad (1)$$

where $H_{\max}$ is the hardness of the CR samples at an annealing temperature where recrystallization starts, $H_{\min}$ is the hardness of completely recrystallized samples, H_i is the hardness value at any particular annealing temperature,

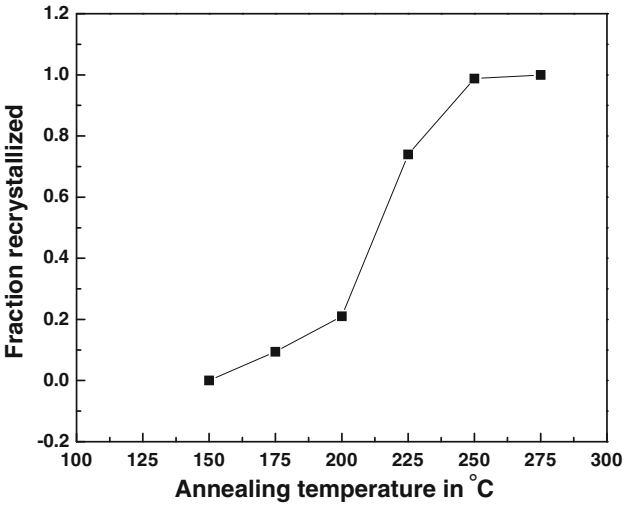

Fig. 10 Variation of fraction recrystallized with annealing temperature obtained from hardness values of CR Al 6063 alloy

and X_i is the fraction recrystallized at particular annealing temperature.

Using the hardness results (Fig. 9) and Eq. 1, the fraction recrystallized at each annealing temperature is calculated and the variation of fraction recrystallized for different annealing temperatures is plotted in Fig. 10. H_{max} and H_{min} values were chosen based on the hardness values corresponding to the annealing temperature of 150 and 275 °C, respectively. At the low-temperature region (150–175 °C), the rate of recrystallized fraction is less. Hence, the microstructural instability is prominent during the early stage of annealing. The middle part of the curve represents a composite microstructure consisting of deformed and recrystallized regions. At higher-temperature annealing (250–275 °C), the curve becomes flat. It indicates that a stable, recrystallized microstructure has formed during high-temperature annealing.

Conclusions

The effect of annealing on precipitation, microstructural stability, and mechanical properties of CR Al 6063 alloy has been studied in details, in the present investigation. The following conclusions are made.

- In the CR samples, before annealing treatment, the microstructure is heavily deformed with diffused, non-equilibrium, and ill-defined grain boundaries. During low-temperature annealing treatment of 150–175 °C, a significant reduction in dislocation density within the grains and at grain boundaries has occurred. Some of the dislocations rearrange themselves to form subgrains and many of the elongated substructure boundaries recovered into subgrain boundaries during recovery process. Above the temperature of 175 °C, the effective recrystallization has started and completed at an annealing temperature 250 °C. The grain growth has occurred at the temperature above 250 °C.
- The precipitate evolution, during annealing of CR Al 6063 alloy, follows as per the sequence: the formation of GP zones, β'' phase, β' phase, and stable β phase have occurred at the annealing temperatures of 150 °C for 1 h, 175 °C for 1 h, 200 °C for 1 h, and 250 °C for 1 h, respectively.
- The morphology of GP zones, β'' phase, β' phase, and stable β phase are spherical, needle, rod, and plate shape, respectively.
- The CR Al 6063 alloy samples are thermally stable at an annealing treatment up to 225 °C. Within the range of 150–225 °C, the small precipitate particles of GP zones, β'' phase, β' phase have formed, whose dimensions are below the range of 1 μm. At high temperatures (250 and 300 °C), growth of the precipitates has occurred in addition to grain coarsening.
- The strength and hardness of the CR samples have gradually improved up to the annealing temperature of 175 °C due to the coherency of precipitates with the matrix. When the temperature is increased beyond 175 °C, the CR sample loses its hardening effect due to the incoherent precipitate particles. At the temperature above 250 °C, there is no change in yield strength, tensile strength, and hardness, which confirms the completion of recrystallization process at 250 °C.

Acknowledgements One of the authors, Dr. Sushanta Kumar Panigrahi, would like to thank CSIR, New Delhi for having supported this work through RA fellowship. Dr. R. Jayaganthan expresses his sincere thanks to DST, New Delhi for their financial grant to this work through Grant no DST-462-MMD.

References

1. Burger GB, Gupta AK, Jeffrey PW, Lloyd DJ (1995) Mater Charact 35:23
2. Usta M, Glicksman ME, Wright RN (2004) Metall Mater Trans A 35A:435
3. Andersen SJ (1995) Metall Mater Trans A 26A:1931
4. Miller WS, Zhuang L, Bottema J, Wittebrood AJ, Smet PD, Haszler A (2000) Mater Sci Eng A 280:37
5. A statistical review on Aluminium Shipments by Major Market, United states and Canada, 2004
6. Wang Y, Chen M, Zhou F, Ma E (2002) Nature 419:912
7. Valiev RZ, Islamgaliev RK, Alexandrov IV (2000) Prog Mater Sci 45:103
8. Panigrahi SK, Jayaganthan R, Pancholi V (2009) Mater Des 30:1894
9. Panigrahi SK, Jayaganthan R, Chawla V (2008) Mater Lett 62:2626
10. Panigrahi SK, Jayaganthan R (2008) Mater Sci Forum 584:734
11. Kim YG, Ko YG, Shin DH, Lee S (2010) Acta Mater 54:2545
12. Kwan C, Wang Z, Kang SB (2008) Mater Sci Eng A 480:148
13. Tsuji N, Ito Y, Saito Y, Minamino Y (2002) Scripta Mater 47:893
14. Kamikawa N, Tsuji N, Huang X, Hansen N (2006) Acta Mater 54:3055
15. Panigrahi SK, Jayaganthan R (2008) Mater Sci Eng A 480:299
16. Mishra RS, Mukherjee AK (1997) Mater Sci Eng A 234:1023
17. Ma Y, Furukawa M, Horita Z, Nemoto M, Valiev RZ, Langdon TG (1996) Mater Trans 37:336
18. Szczygiel P, Roven HJ, Reiso O (2008) Mater Sci Eng A 493:202
19. Lee YB, Shin DH, Park KT, Nam WJ (2004) Scripta Mater 51:355
20. Cao WQ, Godfrey A, Liu W, Liu Q (2004) Mater Lett 51:3667
21. Doherty RD, Hughes DA, Humphreys FJ, Jonas JJ, Jensen DJ, Kassner ME, King WE, McNelley TR, McQueen HJ, Rollett AD (1997) Mater Sci Eng A 234–236:219
22. Rangaraju N, Raghuram T, Krishna BV, Rao KP, Venugopal P (2005) Mater Sci Eng A 398:246
23. Miao WF, Laughlin DE (1999) Scripta Mater 40:873
24. Esmaeili S, Wang SX, Lloyd DJ, Poole WJ (2003) Metall Mater Trans A 34A:751
25. Edwards GA, Stiller K, Dunlop GL, Couper MJ (1998) Acta Mater 46:3893

26. Jacobs MH (1972) Philos Mag 26:1
27. Yassar RS, Cai M, Field DP, Chen X, Asay J (2006) J Mater Sci 41:1711. doi:10.1007/s10853-006-0870-5
28. Yassar RS, Field DP, Weiland H (2005) Metall Mater Trans A 36A:2059
29. Buha J, Lumley RN, Crosky AG, Hono K (2007) Acta Mater 55:3015
30. Urrutia IG, Munoz-Morris MA, Morris DG (2005) Mater Sci Eng A 394:399
31. Humphrey FJ, Prangnell PB, Bowen JR, Gholinia A, Harris C (1999) Philos Trans Roy Soc Lond 357A:1663
32. Morris DG, Munoz-Morris MA (2002) Acta Mater 50:4047
33. Weatherly GC, Perovic A, Mukhopadhyay NK, Llyod DJ, Perovic DD (2001) Metall Mater Trans A 32:213